Biophysical Journal Volume 74 January 1998 559–568

Role of the Scaffolding Protein in P22 Procapsid Size Determination Suggested by $T = 4$ and $T = 7$ Procapsid Structures

Pamela A. Thuman-Commike,*§ Barrie Greene,# Justine A. Malinski,§ Jonathan King,# and Wah Chiu§
*Department of Computational and Applied Mathematics, W. M. Keck Center for Computational Biology, Rice University, Houston, Texas 77005-1892; #Department of Biology, Massachusetts Institute of Technology, Cambridge, Massachusetts 02139; and §Verna and Marrs McLean Department of Biochemistry, Baylor College of Medicine, Houston, Texas 77030 USA

ABSTRACT Assembly of bacteriophage P22 procapsids requires the participation of ~300 molecules of scaffolding protein in addition to the 420 coat protein subunits. In the absence of the scaffolding, the P22 coat protein can assemble both wild-type-size and smaller size closed capsids. Both sizes of procapsid assembled in the absence of the scaffolding protein have been studied by electron cryomicroscopy. These structural studies show that the larger capsids have $T = 7$ icosahedral lattices and appear the same as wild-type procapsids. The smaller capsids possess $T = 4$ icosahedral symmetry. The two procapsids consist of very similar penton and hexon clusters, except for an increased curvature present in the $T = 4$ hexon. In particular, the pronounced skewing of the hexons is conserved in both sizes of capsid. The $T = 7$ procapsid has a local non-icosahedral twofold axis in the center of the hexon and thus contains four unique quasi-equivalent coat protein conformations that are the same as those in the $T = 4$ procapsid. Models of how the scaffolding protein may direct these four coat subunit types into a $T = 7$ rather than a $T = 4$ procapsid are presented.

INTRODUCTION

Under the principles of quasi-equivalence theory (Caspar and Klug, 1962), the assembly of viruses containing more than 60 coat protein subunits requires conformational switching of the subunits to different quasi-equivalent conformations. The total number of subunits within an icosahedral virus capsid is $T \times 60$, where T is the number of quasi-equivalent conformations. Thus conformational switching is intimately related to determination of capsid size, a critical issue, because the capsid must be large enough to encapsulate the entire viral genome. Various mechanisms of conformational switching exist (Johnson, 1996).

Size regulation by conformational switching is well understood for smaller viruses, such as the $T = 3$ RNA viruses (Rossmann and Johnson, 1989; Johnson, 1996). In several of these viruses, switching is regulated by a terminal protein segment that adopts an ordered conformation in one subunit type (Harrison et al., 1978; Abad-Zapatero et al., 1980; Fisher and Johnson, 1993). The presence or absence of this structured polypeptide segment affects subunit interactions at the quasi-twofold contacts, determining whether these contacts will be either flat or bent. When this regulatory segment is removed by proteolytic cleavage, the protein can form only $T = 1$ capsids in which all contacts are bent (Erickson and Rossmann, 1982). In some $T = 3$ viruses, ordered RNA makes up part of the switch (Fisher and Johnson, 1993; Wery et al., 1994).

The structure of the nominally $T = 7$ papilloma virus SV40 reveals that contacts between subunits of different capsomeres are also regulated by conformational switching in a C-terminal arm of the coat protein (Liddington et al., 1991). The lattice of SV40, however, differs from the quasi-equivalent model in that both pentavalent and hexavalent positions are occupied by pentamers (Liddington et al., 1991). Thus the conformational switching mechanisms observed in this structure are probably not a general model for other classes of $T = 7$ viruses.

The conformational switching of larger viruses, such as the double-stranded DNA bacteriophages ($T = 7$), herpesviruses ($T = 16$), and adenoviruses ($T = 25$), appears to be more complex, and its mechanism is currently unknown. These viruses have assembly pathways that proceed through the formation of a non-DNA-containing precursor capsid (Casjens and Hendrix, 1988; Rixon, 1993; Edvardsson et al., 1976; D'Halluin et al., 1978). In place of the DNA, these procapsids contain up to several hundred molecules of scaffolding proteins, which are required for assembly but are not found in the mature virions. The functions of scaffolding proteins have been particularly well characterized for the dsDNA phages, including the coliphages T4, T3, T7, P2, and λ; the *Bacillus subtilis* phage Φ29; and the *Salmonella typhimurium* phage P22 (Casjens and Hendrix, 1988). Possible functions of scaffolding proteins include capsid morphogenesis (Casjens and Hendrix, 1988; Kellenberger, 1990), organization of a specialized portal complex required for DNA packaging and injection (Murialdo and Becker, 1978; Greene and King, 1996), exclusion of cellular proteins from within the assembling capsid (Earnshaw and

Received for publication 13 March 1997 and in final form 10 July 1997.

Address reprint requests to Dr. Pamela A. Thuman-Commike, Vera and Marrs McLean Department of Biochemistry, Baylor College of Medicine, One Baylor Plaza, Houston, TX 77030. Tel.: 713-798-6989; Fax: 713-796-9438; E-mail: pthuman@caam.rice.edu.

Dr. Greene's present address is Department of Microbiology and Immunology, School of Medicine, and G. W. Hooper Foundation, University of California San Francisco, San Francisco, CA 94143-0552.

Dr. Malinski's present address is ATG Laboratories, 10300 Valley View Rd., No. 107, Eden Prairie, MN 55344.

0006-3495/98/01/559/10 $2.00

Casjens, 1980), and DNA packaging (King and Chiu, 1997). It is believed that the scaffolding proteins may also play a critical role in size regulation (Kellenberger, 1990).

For bacteriophage P22, participation of 200–300 scaffolding subunits in addition to the 420 coat protein subunits is required for intracellular assembly of a $T = 7$ procapsid. The procapsid also includes a dodecameric portal complex that serves as the site for DNA entry (Bazinet and King, 1988), as well as several copies each of pilot proteins required for DNA injection into the host cell (King et al., 1973). Incorporation of the portal and pilot proteins occurs early in procapsid assembly (Bazinet and King, 1988; Thomas and Prevelige, 1991), and these proteins may be involved in the formation of an assembly initiation complex (Bazinet et al., 1990). During the process of phage maturation, the scaffolding molecules are released intact from the capsid, probably through the channels present at the hexon centers (Prasad et al., 1993), and are recycled to form new procapsids (King and Casjens, 1974). At this point the DNA is packaged into the capsid and the coat lattice undergoes conformational transitions resulting in expansion, angularization, and closure of the channels (Prasad et al., 1993).

In the absence of scaffolding protein, intracellular assembly of the coat protein is slower (Casjens and King, 1974). Eventually the P22 coat protein within infected cells forms some correctly sized procapsids, but many smaller than normal procapsids and aberrant spiral structures are also produced (Earnshaw and King, 1978). Neither the spirals nor either size of closed capsid contain the portal or pilot proteins (Earnshaw and King, 1978). Consequently, the capsids cannot package DNA and are dead-end products.

The small capsids formed in the absence of scaffolding are of particular interest because the coat proteins of other dsDNA phages, P2 and λ, are also capable of forming both $T = 7$ and smaller capsids. The coat protein of phage P2 can assemble both the P2 capsids and the smaller capsids of the parasitic phage P4 (Lindqvist et al., 1993). Structures of the P2 and P4 mature phages revealed that their capsids are $T = 7$ and $T = 4$, respectively (Dokland et al., 1992). Several point mutations in the coat protein of the $T = 7$ phage λ result in the formation of small capsids (Katsura and Kobayashi, 1990). The structure of these capsids has not been solved, but they are also estimated to be $T = 4$ (Katsura, 1983).

We have previously determined the structure of the wild-type P22 procapsid to 19 Å (Thuman-Commike et al., 1996). At this resolution subunits at different positions have clearly altered conformations, suggesting that more extensive conformational shifts than that of terminal arms are involved. We have determined the structures of both wild-type-size and small capsids formed in the absence of scaffolding protein, in the hope that this would help to illuminate the mechanism of conformational switching between the two capsid sizes and the roles scaffolding might play in this switch. These structures provide the first direct comparison at the procapsid stage of $T = 7$ and $T = 4$ lattices assembled from the same coat protein.

MATERIALS AND METHODS

Capsid preparation

Capsids were prepared from cells infected with phage carrying an amber mutation in the scaffolding gene, 8amH202, resulting in a nonfunctional scaffolding fragment (King et al., 1973). In the absence of scaffolding protein, the coat protein within cells forms some capsids that are the size of normal procapsids but are empty of scaffolding protein, as well as smaller filled capsids and large spiral structures (Earnshaw and King, 1978). These structures were purified according to previously described protocols for procapsid purification (Prevelige et al., 1988; Thuman-Commike et al., 1996). The infection was carried out at 40°C rather than 35°C because the proportion of small capsids produced increases with temperature (Greene and King, 1996). After purification, the structures were applied to a Bio-Gel A-50m column to separate the spirals from the wild-type-size and small closed capsids (Earnshaw and King, 1978). The column fractions were assayed by absorbance at both 280 and 330 nm measured in a Gilford spectrophotometer. Two approximately equal peaks were observed by absorbance at 280 nm. The earlier eluting peak had a much higher level of light scattering, as seen by absorbance at 330 nm, confirming that this peak contained the large spiral structures. Fractions from the second peak, containing the wild-type-size and small capsids, were pelleted by centrifugation for 50 min at 35,000 rpm in a Beckman 45Ti rotor and resuspended to a concentration of ~10 mg/ml.

Electron cryomicroscopy

Capsid samples were applied to copper grids covered with holey carbon film that was glow-discharged immediately before use (Fukami and Adachi, 1965). After removal of excess solution by blotting, the grid was rapidly plunged into liquid ethane (Adrian et al., 1984; Dubochet et al., 1988). Vitrified samples were stored under liquid nitrogen until transfer into a JEOL 1200 microscope equipped with a Gatan 651-N anticontaminator, maintained at −179°C, and a Gatan 626 cold stage, maintained at −165°C. Images were obtained with 100-kV electrons at a magnification of 30,000 under low-dose conditions (less than or equal to 5 $e^-/Å^2$) and were recorded on Kodak SO-163 film. The film was developed in full-strength Kodak D19 for 12 min at 20°C and fixed for 10 min in Kodak fixer.

Image analysis and three-dimensional reconstruction

Electron micrographs were visually inspected for image quality, ice quality, and number of capsids per micrograph. The close-to-focus images of two suitable micrographs were scanned using a Perkin-Elmer 1010M microdensitomer with a step size of 17 μm, which corresponds to 5.57 Å per pixel in the scanned image. Particle selection was performed interactively to allow particle images to be divided into the four capsid classes based on size. All selected particles were perimeter average subtracted and extracted as 128 × 128 pixel images. The selected particle images were then analyzed by computing the sum of the Fourier transform intensities to ensure the images did not contain drift or astigmatism and to evaluate the defocus value (Zhou et al., 1996).

Initial particle centers were estimated as the center of gravity of the cross-correlation peak between a particle and a rotationally averaged reference (Thuman-Commike and Chiu, 1997). The particles were then masked with a circular mask slightly larger than the capsid to reduce background noise. Next, for each particle image, an initial set of possible orientations was found by performing a search over the icosahedral asymmetric unit at 1° intervals, using several self-common line functions (Thuman-Commike and Chiu, 1997).

For the small procapsids, a set of five estimated particle orientations with low self-common lines phase residuals were chosen for refinement. These selected particle orientations were refined by using cross-common line phase residual refinement (Crowther et al., 1970; Fuller, 1987) over all

five orientation parameters: ϕ, θ, ω, and the center x, y (Zhou et al., 1994). After refinement the particles were reconstructed to generate an initial low-resolution structure at ~35-Å resolution. Projection images were computed from the low-resolution structure for use as a template to evaluate additional particle orientations by using the cross-common line phase residual (Zhou et al., 1994; Crowther et al., 1994). After identification of additional particle orientations, refinement was performed on all of the particle orientations at increasingly higher resolutions to obtain an improved reconstruction. The cycle of orientation search, five parameter orientation refinement, reconstruction, and template projection was repeated until no further particle orientations were identified.

Orientation determination of the wild-type-size procapsid followed the method outlined above, except that a modified initial particle orientation selection method was used. Rather than select initial particle orientations based on only the value of the self-common line phase residual, a computed projection image template from the previously published 19-Å scaffolding mutant reconstruction (Thuman-Commike et al., 1996) was used to identify an initial set of orientations. All identified orientations were then refined alone without the mutant procapsid template. The refined orientations were reconstructed into a moderate resolution structure (30 Å) for generation of computed projection images. After determination of this initial reconstruction, the orientation determination procedure proceeded as described above.

The final resolution of each reconstruction was verified by the icosahedral cross-common lines phase residual (Crowther, 1971; Stewart et al., 1991), the Fourier ring correlation coefficient between two independent reconstructions (Saxton and Baumeister, 1982; van Heel et al., 1982; Radermacher, 1988), and the amplitude-weighted mean phase difference between two independent reconstructions (Frank et al., 1981; Baker et al., 1990). To ensure adequate Fourier space sampling, the inverse eigenvalue spectrum was calculated during the interpolation step of the Fourier Bessel analysis of the final reconstructions (Crowther et al., 1970; Crowther, 1971). Full icosahedral symmetry was obtained for the final reconstructions by imposing real-space threefold averaging (Fuller, 1987). These structures were then analyzed to determine if the inner cores were icosahedral, using previously described methods (Thuman-Commike et al., 1996) that compare the non-threefold averaged density map with the threefold averaged density map as a function of radius.

RESULTS

Capsid preparation

Capsids assembled in the absence of the scaffolding protein were purified as described in Materials and Methods. The protein composition of these particles was analyzed by sodium dodecyl sulfate-polyacrylamide gel electrophoresis (Fig. 1). These capsids clearly lack the scaffolding protein, as shown by comparison to procapsids assembled in the presence of scaffolding protein. They also do not appear to contain the portal protein or either of the two pilot proteins gp16 and gp20. These particles do include small amounts of four proteins that are not found in wild-type procapsids. One of these proteins was previously identified as the P22 tailspike protein, whereas the others are presumably host cell proteins (Earnshaw and King, 1978). The 67-kDa protein may be a host chaperone. Analysis of purified small and wild-type-size capsids demonstrated that the additional proteins are found in both sizes of capsid (Earnshaw and King, 1978); thus there is no evidence that they are important in size determination.

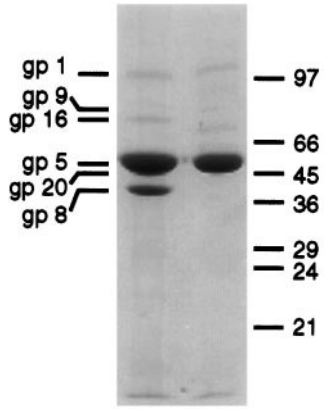

FIGURE 1 Protein composition of P22 procapsids assembled in the presence and absence of the scaffolding protein. Procapsid samples were analyzed by sodium dodecyl sulfate-polyacrylamide gel electrophoresis on a 12% polyacrylamide gel; the gel was stained with Coomassie blue. *Left lane*: Wild-type procapsids. *Right lane*: Capsids produced by the scaffolding-minus strain. Each lane contains 2.5 μg total protein. Positions of the P22 coat protein (gp5), scaffolding protein (gp8), portal protein (gp1), pilot proteins (gp16 and gp20), tailspike protein (gp9), and molecular weight markers are shown. Note that the scaffolding protein typically migrates anomalously to a position higher than predicted by its molecular weight.

Electron cryomicroscopy and three-dimensional reconstruction

Two electron micrographs at defocus values of 1.0 and 1.1 μm underfocus (Fig. 2) were selected and processed as described in Materials and Methods. As with previous stud-

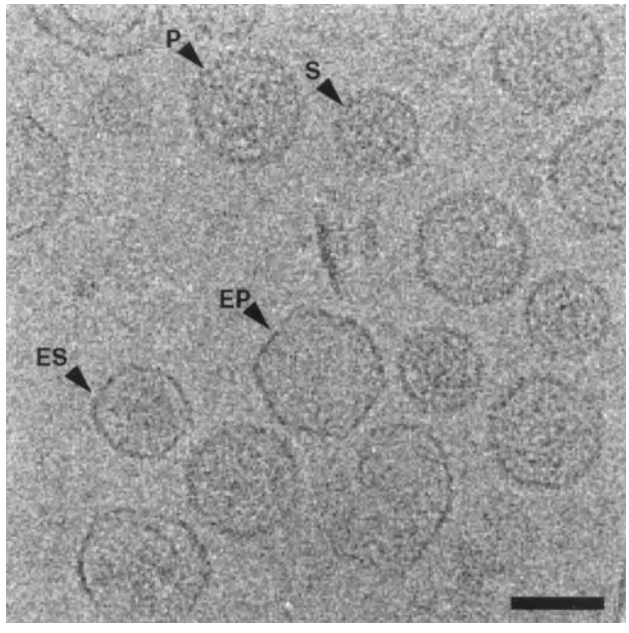

FIGURE 2 Selected region of a 1.1-μm underfocus 100-kV flood-beam micrograph of procapsids assembled in the absence of the scaffolding procapsid. S denotes small procapsids, ES enlarged small procapsids, P wild-type sized procapsids, and EP enlarged wild-type-size procapsids. Also present in this region are aberrant and spiral-like particles. Scale bar, 500 Å.

ies of procapsids assembled in the absence of scaffolding protein (Earnshaw and King, 1978), capsids similar in size to wild-type procapsids, a smaller procapsid, and aberrant spirals are present. Unlike in the previous studies, however, two additional classes are present that appear to be enlarged versions of both the small and wild-type-size procapsids (Fig. 2). These enlarged capsids are significantly more angular, have thinner shells, and appear empty in comparison to the corresponding nonenlarged procapsids. Specifically, the enlarged wild-type-size capsid has the same diameter and resembles the appearance of the mature phage (Prasad et al., 1993). Presumably, these capsids have undergone maturation expansion in the absence of DNA. It was previously shown that the wild-type-size capsids assembled in the absence of the scaffolding protein are capable of undergoing expansion in vitro, as do wild-type procapsids (Earnshaw and King, 1978), but this is the first demonstration that the small procapsid lattice can undergo a comparable transition. Preliminary processing indicates that both of these enlarged capsids are icosahedral. However, three-dimensional structural studies were not pursued at this time because only a small number of these capsids are present.

The small and wild-type-size procapsids were processed, resulting in reconstructions at a nominal resolution of 22 Å, as assessed by all three resolution determination methods described in Materials and Methods. The small procapsid structure includes 76 particle images, with 94% of the mean inverse eigen values less than 0.01 and none greater than 0.1. The wild-type-size procapsid structure includes 147 particle images, with 97% of the mean inverse eigen values less than 0.01 and none greater than 0.1.

Three-dimensional structure of small and wild-type-size procapsids

The small procapsid structure possesses a $T = 4$ icosahedral lattice with an average radius of 195 Å and a maximum radius of 240 Å (Fig. 3, *a* and *b*). In contrast to the $T = 4$ lattice of the small procapsid, the wild-type-size procapsid reconstruction forms a $T = 7$ icosahedral lattice (Fig. 3, *c* and *d*), which is very similar to the wild-type procapsid assembled in the presence of the scaffolding protein (Thuman-Commike et al., 1996). The average radius of the wild-type-size procapsid is 260 Å, with a maximum radius of 306 Å. Both the $T = 4$ and $T = 7$ procapsids have an ~85-Å-thick outer icosahedral shell, which is attributed to the 47-kDa coat protein gp5.

Two layers of density are present in both the $T = 4$ and the $T = 7$ reconstructions (Fig. 4). These inner cores may be composed of additional coat proteins or the minor proteins observed in the gel in Fig. 1. One proposed function of the scaffolding protein in wild-type procapsids is to prevent the inclusion of cellular components in the procapsid (Earnshaw and Casjens, 1980). This may explain why the minor proteins are not observed in wild-type procapsids. Comparison of both reconstructions before and after applying icosahedral threefold symmetry confirms that neither inner core density is icosahedral.

Features of small and wild-type-size procapsids

Despite the different sizes and *T* numbers of the two procapsids, their overall structural features are quite similar (Fig. 3, *a–d*). Both procapsids are composed of penton and

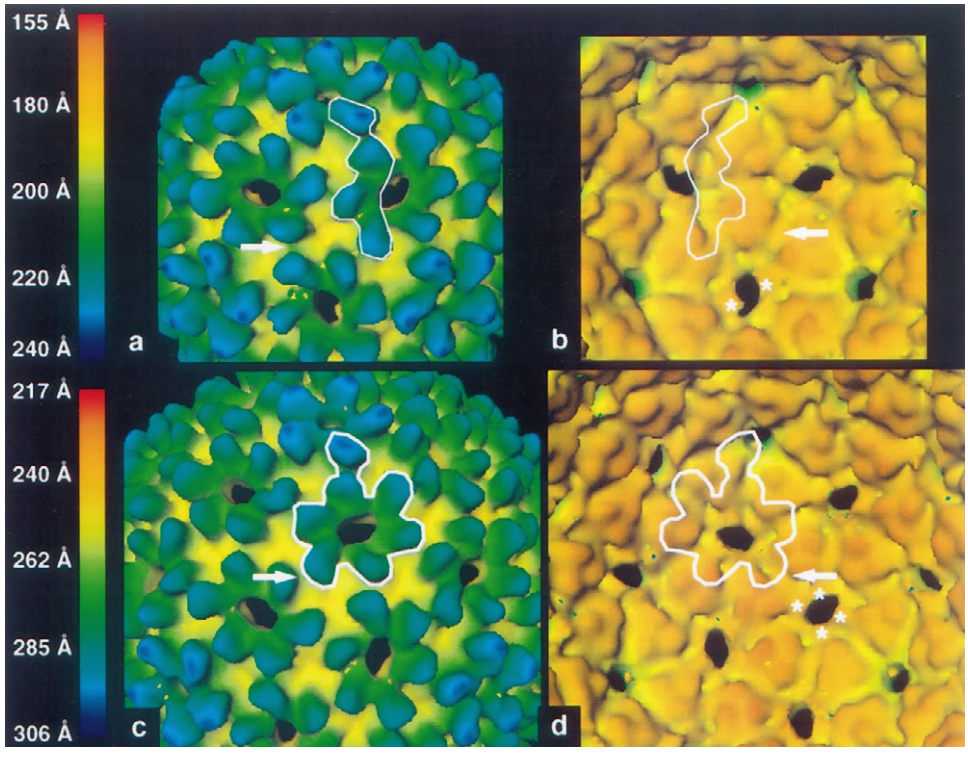

FIGURE 3 Color-coded surface representations of small and wild-type-size procapsids. (*a* and *b*) Inner and outer surfaces of the small procapsid; (*c* and *d*) wild-type-size procapsid. The surface is color coded such that densities that extend inward the most are red, and those that extend outward the most are blue; see scale bars. The arrows indicate the regions connecting neighboring hexons and pentons, which are elevated bridges or saddle-like regions on the outer surface and appear as grooves on the inner surface. The asterisk's indicate the fingerlike regions at the edge of the hexon. In addition, the asymmetric unit of each procapsid is outlined.

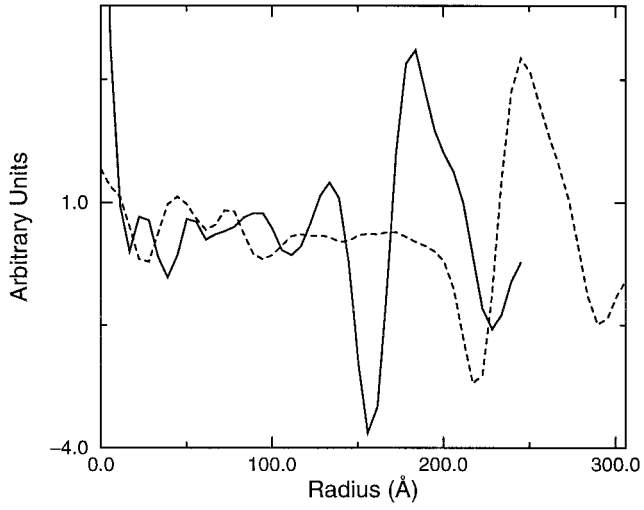

FIGURE 4 Radial density plots of the small and wild-type-size procapsid.

skewed hexon clusters with the same overall dimensions in each procapsid. As with the previously studied procapsid structure (Thuman-Commike et al., 1996), the hexons have four fingerlike densities protruding inward from the edge of each hexon hole (Fig. 3, *b* and *d*). These densities, however, are less prominent at this resolution than in the 19-Å procapsid structure. In addition, in the $T = 4$ procapsid only two densities appear to be present. The regions connecting neighboring hexons and pentons on the outer surface (Fig. 3, *a* and *c*) appear as depressions at all strict and local icosahedral threefold axes, and as elevated bridges or saddlelike regions between neighboring hexon-hexon and hexon-penton subunit pairs. On the inner surface (Fig. 3, *b* and *d*) the depressions at all strict and local icosahedral threefold axes appear as knobs, and the bridges between hexon-hexon and hexon-penton subunit pairs appear as a network of grooves.

Comparison of small and wild-type-size procapsid lattices and subunit interactions

The $T = 4$ small procapsid contains four quasi-equivalent subunits (labeled *A–D* in Fig. 5 *a*), and the $T = 7$ wild-type-size procapsid contains seven quasi-equivalent subunits (labeled *A–G* in Fig. 5 *b*). However, as with the wild-type $T = 7$ procapsid (Thuman-Commike et al., 1996), this $T = 7$ procapsid contains a local non-icosahedral twofold axis that does not intersect the center of the icosahedron, as confirmed by superimposing each compuationally isolated hexon with a 180° rotated version of itself. Because the B, C, and D subunits are equivalent to the E, F, and G subunits, the $T = 7$ lattice contains only four unique quasi-equivalent subunits at the current resolution. For clarity, the

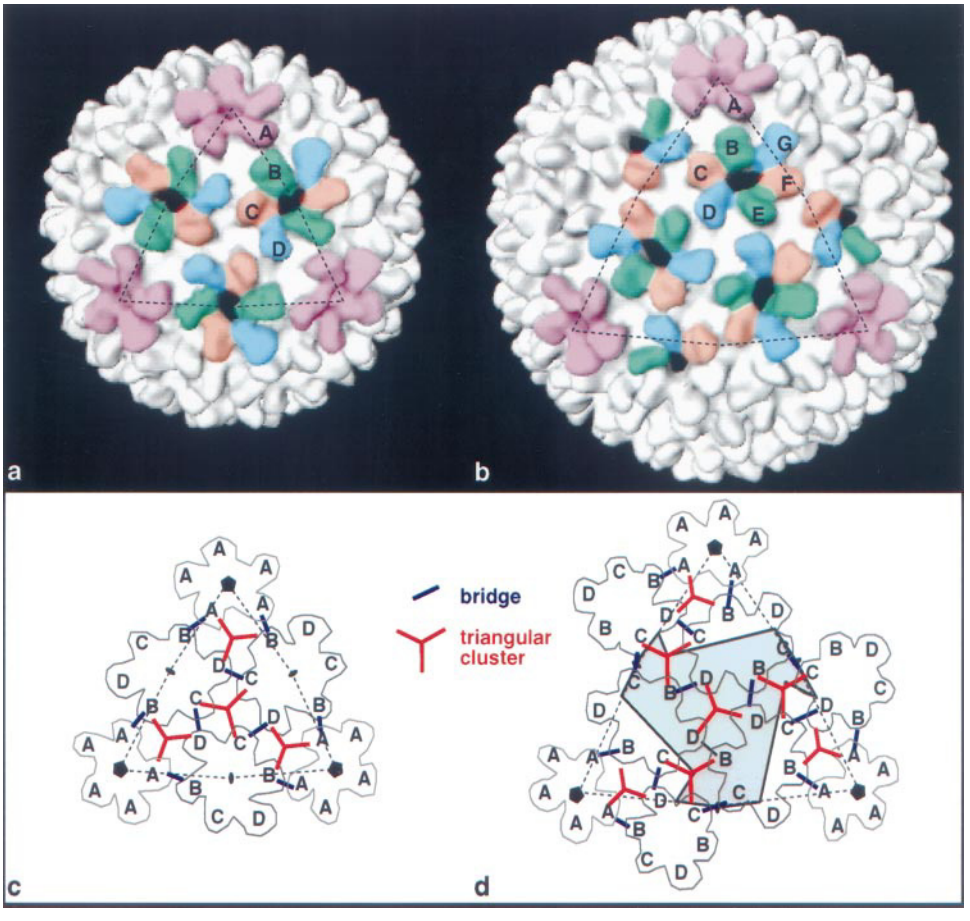

FIGURE 5 Schematic icosahedral lattices and subunit interactions of the $T = 4$ and $T = 7$ procapsids. Surface representations of the (*a*) small procapsid and (*b*) wild-type-size procapsid, with all of the quasi-equivalent subunits in one asymmetric unit labeled. The four unique quasi-equivalent subunits found in both procapsids are color coded. (*c*) Small and (*d*) wild-type-size procapsid unit triangles with the bridge and triangular cluster interactions denoted. The four unique quasi-equivalent subunits are labeled. In addition, the unique region of the wild-type-size procapsid is highlighted.

labels for E, F, and G in the schematic diagram of Fig. 5 *d* have been replaced with B, C, and D. Notice, however, that the interactions that occur between the equivalent subunits and other hexon or penton subunits are different. That is, the equivalence of the B, C, and D subunits to the E, F, and G subunits is restricted to subunit conformations and does not include the subunit interactions.

The quasi-equivalent subunits of the procapsid lattices interact with each other in two distinct manners (Fig. 5, *c* and *d*), as described earlier. The first type of interaction is the pairwise bridges between subunit pairs in neighboring hexon or penton clusters (*blue interactions* in Fig. 5, *c* and *d*). In the small procapsid these pairwise interactions occur between the AB and CD subunits. In the wild-type-size procapsid two additional interactions occur between the BD and the CC subunits. The second type of interaction is the triangular clusters at strict and local threefold axes (*red interactions* in Fig. 5, *c* and *d*). In the case of the small procapsid, these interactions occur between three C subunits (CCC) and between the A, B, and D subunits (ABD). In the case of the wild-type-size procapsid, the ABD interactions also occur. However, the CCC interactions do not occur in the $T = 7$ procapsid; rather, interactions occur between three D subunits (DDD) and two C subunits with one B subunit (CCB). Notice that the four different interactions observed in the $T = 7$ procapsid all occur between the second half of each hexon, as denoted in the shaded region of Fig. 5 *d*. At this resolution, structural differences in these various interactions are not observed.

As suggested by the similarities in lattice interactions, the penton and surrounding hexons of the two procapsids are very similar to each other but differ in placement within the icosahedral lattice. That is, the small procapsid pentons lie at a different angle of rotation with respect to the wild-type-size procapsid. Alignment of the pentons occurs when the small procapsid is rotated 50° about the fivefold axis. In Fig. 6 the difference map between computationally extracted and aligned fivefold regions of the small and wild-type-size procapsids is shown. Notice that although the quasi-equivalent subunits of each capsid are very similar, at this resolution, the hexons possess a change in curvature (see *arrows* in Fig. 6) as a result of the smaller size of the $T = 4$ capsid. The pentamers of the $T = 4$ and $T = 7$ capsids are virtually identical, as is the conformation of the B subunits that contact the pentameric A subunits. Furthermore, the C and D subunits have the same overall conformations in each procapsid but are positioned at different orientations on each hexon. Thus, at this resolution, the four quasi-equivalent subunits present in the $T = 4$ and the $T = 7$ procapsids exhibit the same conformations.

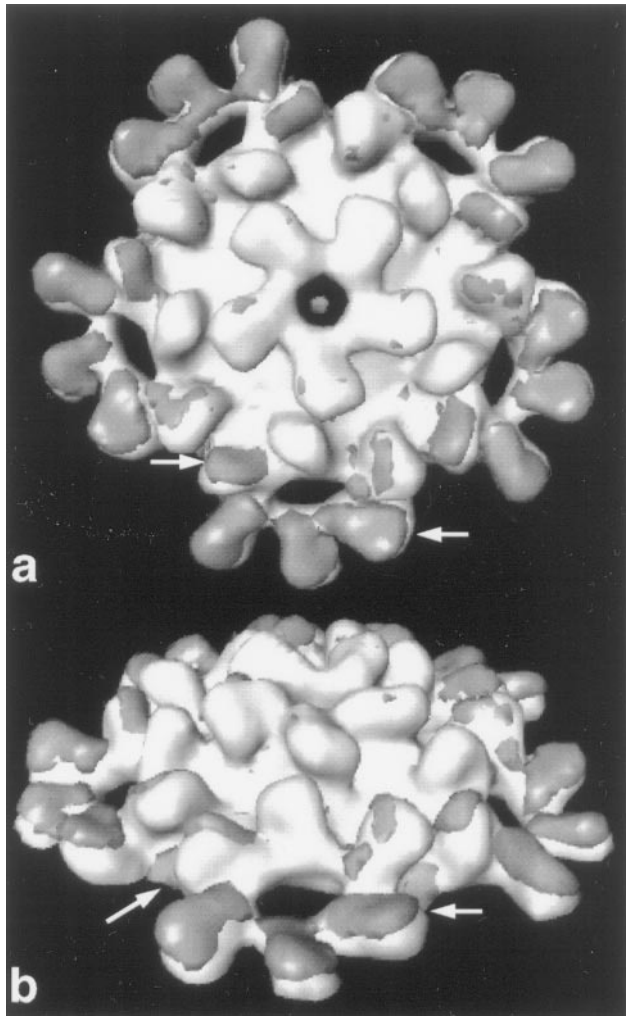

FIGURE 6 Comparison of computationally isolated fivefold views of small and wild-type-size procapsids. The small procapsid is the surface rendered in white. The gray surface is the difference map between the fivefold view of the small procapsid and wild-type-size procapsid. (*a*) Top and (*b*) side view. Although the hexons and pentons of each capsid are very similar, notice that the small capsid hexons have a different curvature, as pointed out by the arrows.

DISCUSSION

Scaffolding protein appears to play an important role in the regulation of the conformational switching involved in directing the assembly of the different quasi-equivalent coat protein conformations required to build a correctly sized P22 procapsid. In the absence of scaffolding, the P22 coat protein forms capsids of two different sizes. We have shown that the wild-type-size capsids produced by the P22 coat protein in the absence of scaffolding protein are $T = 7$, as are wild-type procapsids (Prasad et al., 1993), whereas the small capsids are $T = 4$, as previously predicted from low-angle x-ray scattering data (Earnshaw and King, 1978). The ability to form both $T = 7$ and $T = 4$ capsids is also found in the phage P2 coat protein, gpN, and the phage λ coat protein. In phage P2, wild-type virions are $T = 7$, but the action of gpSid produced by the parasitic phage P4 induces gpN to form $T = 4$ capsids, sufficient in size to package P4 DNA while excluding the larger P2 genome (Lindqvist et al., 1993). In the absence of either gpSid or the P2 scaffolding protein gpO, gpN can form both sizes of

capsid (Marvik et al., 1994). In bacteriophage λ, single amino acid substitutions in the coat protein can result in the production of small capsids, estimated to be $T = 4$ instead of the wild-type $T = 7$ (Katsura, 1983; Katsura and Kobayashi, 1990). Thus there appears to be some structural relationship between $T = 7$ and $T = 4$ lattices such that the coat proteins of $T = 7$ phages are intrinsically capable of forming both these sizes of capsid, but not those of larger or smaller T numbers.

Quasi-equivalence of coat protein subunits

The principles of quasi-equivalence (Caspar and Klug, 1962) imply that the number of distinct subunit conformations within a capsid lattice is the same as the T number; thus construction of a $T = 7$ capsid would require three novel coat subunit conformations that do not exist in a $T = 4$ capsid. The structure of the $T = 4$ P22 capsid reveals the expected four distinct coat subunit types, classified as A–D. The coat subunits of the $T = 7$ P22 capsid are labeled as A–G, with conformations A, B, C, and D corresponding to the four subunits of the $T = 4$ capsid, and with conformations E, F, and G being the conformations that, under the rules of quasi-equivalence, would be novel. Because of the presence of a local twofold axis in the hexamers, however, the conformations of the E, F, and G subunits are equivalent to the conformations of the B, C, and D subunits. Thus the $T = 7$ capsid is assembled using only the same four quasi-equivalent conformations required to build the $T = 4$ capsid.

The presence of a system where only four quasi-equivalent subunit conformations are required to build both $T = 4$ and $T = 7$ capsids does not strictly comply with the rules of quasi-equivalence. Recently, however, a theory of local rules-based assembly has been developed in which the capsid assembly pathway depends only on the interaction of coat subunits with their immediate neighbors, rather than on building blocks such as hexamers and pentamers (Berger et al., 1994). It is possible to devise a set of local assembly rules which direct the assembly of a $T = 7$ capsid from only four different subunit conformations. According to these rules, to prevent formation of a $T = 4$ lattice, the C trimer interaction (see Fig. 5 *c*) must be forbidden (Berger et al., 1994). This might occur if this interaction were of higher energy than the corresponding CCB interaction found in the wild-type-size structure. It may be significant that the percentage of small capsids is higher at 40°C than at 30°C, whereas the percentage of spirals, which can result from substituting a hexamer at a pentameric site, is highest at 17°C (Greene and King, 1996). This interaction might also be blocked by the presence of scaffolding subunits, as discussed below.

Hexon skew

To form a $T = 4$ rather than a $T = 7$ lattice, the coat proteins must alter in conformation to give a larger curvature. This could occur either by hinge-bending motions in the individual coat subunits, so that each one curved slightly more, or by larger scale alterations in hexon shape. In the case of P2/P4, both mature phage structures have been solved to 45-Å resolution (Dokland et al., 1992). The shift to the smaller capsid does result in altered hinge angles of several coat subunits as well as small changes in hexamer geometry (Dokland et al., 1992). The P22 coat subunits also display slightly increased bending, resulting in increased curvature of the small capsid. At this resolution, however, it is clear that the hexons are remarkably similar in the two sizes of capsid. In particular, the distinctive hexon skew is not altered.

All $T = 7$ phages for which procapsid structures have been obtained—P22 (Prasad et al., 1993), λ (Dokland and Murialdo, 1993), and HK97 (Conway et al., 1995)—display skewed hexons that adopt a significantly more symmetrical arrangement upon transition to the mature form. The significance of this skew is unknown, although it is assumed to play some role in the assembly mechanism. The structures presented here are the first that allow direct comparison between $T = 4$ and $T = 7$ lattices at the procapsid stage. These structures demonstrate that hexon skewing is not sufficient to regulate the capsid size of P22, because the same skewed hexons are found in the $T = 4$ as well as the $T = 7$ capsids.

The $T = 4$ P22 procapsid structure displays differences from the $T = 4$ P4 procapsid, suggesting that it is not generated by a comparable morphological mechanism. In the case of P4, the axis of the hexamer is coincident with the capsid twofold axis (Marvik et al., 1995), rather than being offset by an angle, as is observed for the P22 small procapsid. This alignment of the P4 hexamers is undoubtedly influenced by the external scaffolding protein gpSid, which binds directly across the twofold axis of the elongated hexamers (Marvik et al., 1995). The $T = 4$ P22 procapsid includes no equivalent of gpSid, which may explain why the hexamers are not forced into a more symmetrical arrangement. Although the structure of the $T = 7$ P2 procapsid has not been determined, structures of the mature P2 and P4 lattices reveal differences in hexamer geometry (Dokland et al., 1992), which are most likely established at the procapsid stage. It is interesting that whereas binding of gpSid directs formation of the $T = 4$ P4 procapsid, conformational changes analogous to those presumably induced by gpSid do not appear to be required to build the $T = 4$ P22 procapsid.

Capsid size regulation

Role of the scaffolding protein

There is ample evidence that the scaffolding proteins of dsDNA phages play an important role in size regulation. For example, whereas the size and shape of the prolate phage T4 are affected by mutations in a number of different phage proteins, the only mutations that affect capsid width, rather

than length, are those in one of the T4 scaffolding proteins (Kellenberger, 1990). This suggests a special role for the scaffolding proteins in regulating the *T* number, which sets the capsid width. In the case of the isometric P22, the presence of wild-type scaffolding protein sharply reduces the number of small capsids, from 25% of all the structures produced to only 1.5% (Earnshaw and King, 1978).

There are several levels at which scaffolding proteins might regulate capsid size. The scaffolding subunits could bind to individual coat subunits, influencing their conformational switching, or bind at junctions of capsomeres to influence the placement of pentons and hexons. It is also possible that the scaffolding molecules might regulate capsid size by using a simple steric mechanism to affect overall capsid curvature.

The P22 scaffolding molecule is an elongated rod, with estimated dimensions of 247-Å length and 22-Å diameter (Parker et al., 1997). Assuming that the scaffolding molecules are arranged radially, their presence would block the formation of a $T = 4$ capsid, because the radius of this capsid is too small to allow the scaffolding subunits to fit. In this way, the binding of scaffolding to coat subunits during assembly would force them into the wider curvature of the $T = 7$ capsid. This mechanism does not explain, however, the assembly of small capsids from mutant coat proteins of phage λ. These small capsids include small scaffolding cores, containing a reduced number of scaffolding subunits (Katsura, 1983). Because the λ scaffolding protein is only a third the size of the P22 scaffolding, it is reasonable that it can fit within the smaller capsids, but this implies that mechanisms other than steric hindrance help ensure the production of normally sized λ procapsids.

The scaffolding protein could play a more active role in determining capsid size by directly influencing the types of contacts made by the coat subunits. Procapsid assembly is thought to initiate with a pentamer of coat protein (Prevelige et al., 1993). As can be seen in Fig. 5, *c* and *d*, the initial types of coat subunit interactions, from the pentamer to the first surrounding ring of hexamers, are identical between the wild-type-size and small capsids. The next subunits to add would determine the capsid size, based on whether they make the unique interactions of the $T = 7$ capsid. In particular, the C subunits form a trimeric interaction at the threefold axis of the $T = 4$ capsid, but make a dimeric bridge across the twofold axis of the $T = 7$ capsid. Scaffolding molecules form dimers and tetramers, but not trimers, in solution (Parker et al., 1997). Interactions between scaffolding molecules bound to the C coat subunits might force these subunits into a twofold rather than a threefold interaction, thus directing the assembling lattice into the $T = 7$ form.

Last, the scaffolding protein could also affect size determination at a later assembly step, such as the point at which the coat subunits must choose to form either a penton, ensuring production of a $T = 4$ capsid, or another hexon, to form the $T = 7$ capsid. The P2 internal scaffolding, gpO, was proposed to bind at the threefold junction of three hexamers, forming "groups of three" subassemblies that would form the face of a $T = 7$ capsid (Marvik et al., 1995). Although P22 does not appear to assemble via hexameric intermediates or other subassemblies (Prevelige et al., 1993), it is possible that the addition of scaffolding subunits to a growing shell at the appropriate sites could lock in a "group of three" type arrangement. This would forestall the incorporation of a penton at the site required for a $T = 4$ capsid.

Role of the portal

In addition to lacking scaffolding protein, procapsids produced in the absence of scaffolding also fail to incorporate the portal protein. Expression of the portal protein of the prolate phage Φ29 is required to form procapsids of uniform size (Guo et al., 1991). The portal does not play an equally significant role in the assembly of the isometric $T = 7$ phages, because capsids of the correct size are formed in the absence of portals (King et al., 1973; Ray and Murialdo, 1975; Serwer and Watson, 1982). However, P22 scaffolding mutants that prevent incorporation of the portal, as well as minor pilot proteins, produce a higher proportion of small capsids than observed with wild-type, ~5% of the total structures (Greene and King, 1996). It is possible that the portal protein helps to set the initial procapsid curvature, as proposed for Φ29 (Guo et al., 1991). This seems less likely for P22, as the pentamer and surrounding subunits, which would be in contact with the portal, are the most highly conserved regions between the $T = 4$ and $T = 7$ structures. Alternatively, the portal, in a complex with the pilot proteins, may serve as a procapsid initiating center into which scaffolding subunits are recruited (Bazinet et al., 1990); thus in the absence of portals, more capsids are made without the assistance of scaffolding, and form incorrectly.

CONCLUSIONS

A recurring theme in bacteriophage assembly appears to be the regulation of capsid size by the scaffolding protein. The mechanism by which this regulation occurs, however, does not appear to be consistent from phage to phage. In the case of P22, we have shown that in the absence of scaffolding, the P22 coat protein forms both wild-type-size $T = 7$ and smaller $T = 4$ capsids, both of which are composed of the same four unique quasi-equivalent subunits. Thus the scaffolding protein appears to be involved in directing the interactions of the different quasi-equivalent coat protein conformations, so as to ensure the assembly of a correctly sized P22 procapsid. We have presented several models by which the scaffolding proteins might regulate procapsid size. The scaffolding subunits could bind to individual coat subunits, influencing their conformational switching, or bind at junctions of capsomeres to influence the placement of pentons and hexons. Alternatively, scaffolding molecules

might regulate capsid size by using a simple steric mechanism to affect overall capsid curvature.

We thank Dr. B. V. V. Prasad and Dr. Peter E. Prevelige for helpful discussions.

This work was supported by the W. M. Keck Foundation, the National Institutes of Health (RR02250, AI38469, and GM17980), the National Science Foundation (NSFBIR-9413229 and NSFBIR-9412521), and the Center for Research on Parallel Computation, a National Science Foundation Science and Technology Center (CCR-9120008). JAM thanks Dr. Theodore G. Wensel for his generous support (EY07981).

REFERENCES

Abad-Zapatero, C., S. S. Abdel-Meguid, J. E. Johnson, A. G. W. Leslie, I. Rayment, M. G. Rossmann, D. Suck, and T. Tsukihara. 1980. Structure of southern bean mosaic virus at 2.8 Å resolution. *Nature.* 286:33–39.

Adrian, M., J. Dubochet, J. LePault, and A. W. McDowall. 1984. Cryo-electron microscopy of viruses. *Nature.* 308:32–36.

Baker, T. S., W. W. Newcomb, F. P. Booy, J. C. Brown, and A. C. Steven. 1990. Three-dimensional structures of maturable and abortive capsids of equine herpesvirus 1 from cryo-electron microscopy. *J. Virol.* 64: 563–573.

Bazinet, C., and J. King. 1988. Initiation of P22 procapsid assembly in vivo. *J. Mol. Biol.* 202:77–86.

Bazinet, C., R. Villafane, and J. King. 1990. Novel second-site suppression of a cold-sensitive defect in phage P22 procapsid assembly. *J. Mol. Biol.* 216:701–716.

Berger, B., P. W. Shor, L. Tucker-Kellogg, and J. King. 1994. Local rule-based theory of virus shell assembly. *Proc. Natl. Acad. Sci. USA.* 91:7732–7736.

Casjens, S., and R. Hendrix. 1988. Control mechanisms in dsDNA bacteriophage assembly. *In* The Bacteriophages, Vol. 1. R. Calendar, editor. Plenum Press, New York. 15–91.

Casjens, S., and J. King. 1974. P22 morphogenesis I: catalytic scaffolding protein in capsid assembly. *J. Supramol. Struct.* 2:202–224.

Caspar, D., and A. Klug. 1962. Physical principles in the construction of regular viruses. *Cold Spring Harb. Symp. Quant. Biol.* 27:1–24.

Conway, J. F., R. L. Duda, N. Cheng, R. W. Hendrix, and A. C. Steven. 1995. Proteolytic and conformational control of virus capsid maturation: the bacteriophage HK97 system. *J. Mol. Biol.* 253:86–99.

Crowther, R. A. 1971. Procedures for three-dimensional reconstruction of spherical viruses by Fourier synthesis from electron micrographs. *Philos. Trans. R. Soc. Lond. B.* 261:221–230.

Crowther, R. A., D. J. DeRosier, and A. Klug. 1970. The reconstruction of a three-dimensional structure from projections and its application to electron microscopy. *Proc. R. Soc. Lond. B.* 317:319–340.

Crowther, R. A., N. A. Kiselev, B. Böttcher, J. A. Berriman, G. P. Borisova, V. Ose, and P. Pumpens. 1994. Three-dimensional structure of hepatitis B virus core particles determined by electron cryomicroscopy. *Cell.* 77:943–950.

D'Halluin, J.-C., G. R. Martin, G. Torpier, and P. A. Boulanger. 1978. Adenovirus type 2 assembly analyzed by reversible cross-linking of labile intermediates. *J. Virol.* 26:357–363.

Dokland, T., B. H. Lindqvist, and S. D. Fuller. 1992. Image reconstruction from cryo-electron micrographs reveals the morphopoietic mechanism in the P2–P4 bacteriophage system. *EMBO J.* 11:839–846.

Dokland, T., and H. Murialdo. 1993. Structural transitions during maturation of bacteriophage λ capsids. *J. Mol. Biol.* 233:682–694.

Dubochet, J., M. Adrian, J.-J. Chang, J.-C. Homo, J. Lepault, A. W. McDowall, and P. Schultz. 1988. Cryo-electron microscopy of vitrified specimens. *Q. Rev. Biophys.* 21:129–228.

Earnshaw, W. C., and S. R. Casjens. 1980. DNA packaging by the double-stranded DNA bacteriophages. *Cell.* 21:319–331.

Earnshaw, W., and J. King. 1978. Structure of phage P22 coat protein aggregates formed in the absence of the scaffolding protein. *J. Mol. Biol.* 126:721–747.

Edvardsson, B., E. Everitt, H. Jörnvall, L. Prage, and L. Philipson. 1976. Intermediates in adenovirus assembly. *J. Virol.* 19:533–547.

Erickson, J. W., and M. G. Rossmann. 1982. Assembly and crystallization of a $T = 1$ icosahedral particle from trypsinized southern bean mosaic virus coat protein. *Virology.* 116:128–136.

Fisher, A. J., and J. E. Johnson. 1993. Ordered duplex RNA controls capsid architecture in an icosahedral animal virus. *Nature.* 361:176–179.

Frank, J., A. Verschoor, and M. Boublik. 1981. Computer averaging of electron micrographs of 40S ribosomal subunits. *Science.* 214: 1353–1355.

Fukami, A., and K. Adachi. 1965. A new method of preparation of a self-performated micro plastic grid and its application (i). *J. Electron Microsc.* 14:112–118.

Fuller, S. D. 1987. The $T = 4$ envelope of sindbis virus is organized by interactions with a complementary $T = 3$ capsid. *Cell.* 48:923–934.

Greene, B., and J. King. 1994. Binding of scaffolding subunits within the P22 procapsid lattice. *Virology.* 205:188–197.

Greene, B., and J. King. 1996. Scaffolding mutants identifying domains required for P22 procapsid assembly and maturation. *Virology.* 225: 82–96.

Guo, P., S. Erickson, W. Xu, N. Olson, T. S. Baker, and D. Anderson. 1991. Regulation of the phage Φ29 prohead shape and size by the portal vertex. *Virology.* 183:366–373.

Harrison, S. C., A. J. Olson, C. E. Schutt, F. K. Winkler, and G. Bricogne. 1978. Tomato bushy stunt virus at 2.9 Å resolution. *Nature.* 276: 368–373.

Johnson, J. E. 1996. Functional implications of protein-protein interactions in icosahedral viruses. *Proc. Natl. Acad. Sci. USA.* 93:27–33.

Katsura, I. 1983. Structure and inherent properties of the bacteriophage λ head shell. IV. Small-head mutants. *J. Mol. Biol.* 171:297–317.

Katsura, I., and H. Kobayashi. 1990. Structure and inherent properties of the bacteriophage λ head shell. VII. Molecular design of the form-determining major capsid protein. *J. Mol. Biol.* 213:503–511.

Kellenberger, E. 1990. Form determination of the heads of bacteriophages. *Eur. J. Biochem.* 190:233–248.

King, J., and S. Casjens. 1974. Catalytic head assembling protein in virus morphogenesis. *Nature.* 251:112–119.

King, J., and W. Chiu. 1997. The procapsid to capsid transition in double-stranded DNA bacteriophages. *In* Structural Biology of Viruses. W. Chiu, R. Burnett, and R. Garcea, editors. Oxford University Press, New York. 288–311.

King, J., C. V. Lenk, and D. Botstein. 1973. Mechanism of head assembly and DNA encapsulation in *Salmonella* phage P22. II. Morphogenetic pathway. *J. Mol. Biol.* 80:697–731.

Liddington, R. C., Y. Yan, J. Moulai, R. Sahli, T. L. Benjamin, and S. C. Harrison. 1991. Structure of simian virus 40 at 3.8 Å resolution. *Nature.* 354:278–283.

Lindqvist, B. H., G. Deho, and R. Calendar. 1993. Mechanisms of genome propagation and helper exploitation by satellite phage P4. *Microbiol. Rev.* 57:683–702.

Marvik, O. J., T. Dokland, R. H. Nokling, E. Jacobsen, T. Larsen, and B. H. Lindqvist. 1995. The capsid size-determining protein Sid forms an external scaffold on phage P4 procapsids. *J. Mol. Biol.* 251:59–75.

Marvik, O. J., E. Jacobsen, T. Dokland, and B. H. Lindqvist. 1994. Bacteriophage P2 and P4 morphogenesis: assembly precedes proteolytic processing of the capsid proteins. *Virology.* 205:51–65.

Murialdo, H., and A. Becker. 1978. Head morphogenesis of complex double stranded deoxyribonucleic acid bacteriophages. *Microbiol. Rev.* 42:529–576.

Parker, M. H., W. F. Stafford, III, and P. E. Prevelige, Jr. 1997. Bacteriophage P22 scaffolding protein forms oligomers in solution. *J. Mol. Biol.* 268:655–665.

Prasad, B. V. V., P. E. Prevelige, E. Marietta, R. O. Chen, D. Thomas, J. King, and W. Chiu. 1993. Three-dimensional transformation of capsids associated with genome packaging in a bacterial virus. *J. Mol. Biol.* 231:65–74.

Prevelige, P. E., Jr., D. Thomas, and J. King. 1988. Scaffolding protein regulates the polymerization of P22 coat subunits into icosahedral shells in vitro. *J. Mol. Biol.* 202:743–757.

Prevelige, P. E., Jr., D. Thomas, and J. King. 1993. Nucleation and growth phases in the polymerization of coat and scaffolding subunits into icosahedral procapsid shells. *Biophys. J.* 64:824–835.

Radermacher, M. 1988. Three-dimensional reconstruction of single particles from random and nonrandom tilt series. *J. Electron Microsc. Tech.* 9:359–394.

Ray, P., and H. Murialdo. 1975. The role of gene Nu3 in bacteriophage lambda head morphogenesis. *Virology.* 64:247–263.

Rixon, F. J. 1993. Structure and assembly of herpesviruses. *Sem. Virol.* 4:135–144.

Rossmann, M., and J. Johnson. 1989. Icosahedral RNA virus structure. *Annu. Rev. Biochem.* 58:533–573.

Saxton, W. O., and W. Baumeister. 1982. The correlation averaging of a regularly arranged bacterial cell envelope protein. *J. Microsc.* 127: 127–138.

Serwer, P., and R. H. Watson. 1982. Function of an internal bacteriophage T7 core during assembly of a T7 procapsid. *J. Virol.* 42:595–601.

Stewart, P. L., R. M. Burnett, M. Cyrklaff, and S. D. Fuller. 1991. Image reconstruction reveals the complex molecular organization of adenovirus. *Cell.* 67:145–154.

Thomas, D., and P. Prevelige, Jr. 1991. A pilot protein participates in the initiation of P22 procapsid assembly. *Virology.* 182:673–681.

Thuman-Commike, P., and W. Chiu. 1997. Improved common line-based icosahedral particle image orientation estimation algorithms. *Ultramicroscopy.* 68:231–255.

Thuman-Commike, P., B. Greene, J. Jakana, B. V. V. Prasad, J. King, P. E. Prevelige, and W. Chiu. 1996. Three-dimensional structure of scaffolding-containing phage P22 procapsids by electron cryo-microscopy. *J. Mol. Biol.* 260:85–98.

van Heel, M., W. Keegstra, W. Schutter, and E. van Bruggen. 1982. Arthropod hemocyanin structures studied by image analysis. *In* EMBO Workshop: Structure and Function of Invertebrate Respiratory Proteins. Life Chemistry Reports, Suppl. 1 EMBO Workshop. E. Wood, editor. Harwood Academic Publishers, New York. 69–73.

Wery, J-P., V. S. Reddy, M. V. Hosur, and J. E. Johnson. 1994. The refined three-dimensional structure of an insect virus at 2.5 Å resolution. *J. Mol. Biol.* 235:565–586.

Zhou, Z. H., S. Hardt, B. Wang, M. B. Sherman, J. Jakana, and W. Chiu. 1996. CTF determination of images of ice-embedded single particles using a graphics interface. *J. Struct. Biol.* 116:216–222.

Zhou, Z. H., B. V. V. Prasad, J. Jakana, F. Rixon, and W. Chiu. 1994. Protein subunit structures in the herpes simplex virus A-capsid determined from 400 kV spot-scan electron cryomicroscopy. *J. Mol. Biol.* 242:456–469.